JOURNAL OF CATALYSIS 146, 557–567 (1994)

Switchover of Reaction Paths in the Catalytic Decomposition of Formic Acid on TiO_2(110) Surface

H. Onishi, T. Aruga,[2] and Y. Iwasawa[1]

Department of Chemistry, Graduate School of Science, The University of Tokyo, Hongo, Bunkyo-ku, Tokyo 113, Japan

Received October 4, 1993; revised November 29, 1993

The decomposition reaction of formic acid (DCOOD) was examined on a rutile TiO_2(110) surface in catalytic and noncatalytic conditions. The kinetic behavior of the catalytic reaction was recorded by MS under DCOOD atmosphere of 10^{-6}–10^{-3} Pa at 500–800 K, whereas TDS, LEED, AES, XPS, and UPS were used to chracterize adsorbed species derived from formic acid and their non-catalytic surface reactions under vacuum. Formic acid was dissociated to form formates and hydroxyl groups on TiO_2(110) at 250 K. Bridge formates (0.5 ML) were arranged in a (2 × 1) order below 350 K. Formates (0.1 ML) were desorbed under vacuum at 350 K to relax the (2 × 1) overlayer. The evolution of D_2 was observed at 400 K and assigned to recombination of the hydroxyl groups. Residual formates unimolecularly decompose at 570 K with an activation energy of 120 ± 10 kJ/mol and a pre-exponential factor of $2 \times 10^{9\pm1}s^{-1}$, releasing a mixture of CO, CO_2, D_2, D_2O, and DCOOD in TDS. On the other hand, it was found that TiO_2(110) catalyzed two selective reactions: dehydration and dehydrogenation. TiO_2(110) shows a preference for the dehydrogenation reaction into D_2 + CO_2 below 500 K. This is in contrast to the selective activity for the dehydration to D_2O + CO reported on TiO_2 powder catalysts. The rate of the catalytic dehydration was nearly independent of the pressure of formic acid below 700 K, but increased with surface temperature. An activation energy of 120 ± 10 kJ/mol was again observed in the catalytic dehydration reaction, suggesting that the unimolecular decomposition of formates at the surface is rate controlling. The rate of the catalytic dehydrogenation reaction depended on both the coverage of formate and the pressure of DCOOD, with a small activation energy of 15 ± 10 kJ/mol. The catalytic dehydrogenation reaction is thus suggested to proceed in a bimolecular process of a formate and a DCOOD molecule. A kinetic simulation supports the mechanisms, showing a switchover of the reaction paths by the second reactant molecule. These results are discussed, along with previous works on powder catalysts and single crystals.

[1] To whom correspondence should be addressed.

[2] Present address: Department of Chemistry, Faculty of Science, Kyoto University, Kyoto 606-01, Japan.

INTRODUCTION

Metal oxides are popular materials in catalytic chemistry. Many studies on polycrystalline powder catalysts have revealed that catalytic properties strongly depend on the preparation and the history of catalysts. Chemistry on single crystal surfaces of metal oxides, therefore, attracts attention in the surface science community. Experimental (1–13) and theoretical (14) studies on single crystal surfaces have demonstrated that local coordination around reaction sites controls the reaction of adsorbed species on them. Ti^{4+} cations with multiple coordination vacancy cause the disproportionation of formates (5) and the bimolecular ketonization of acetates (6) on faceted TiO_2(001) surfaces.

Those studies, however, have been focused mainly on the characterization of adsorbates and their noncatalytic reactions under vacuum by means of photoelectron and thermal desorption spectroscopies. Several TDS studies already observed the decomposition of formates on TiO_2 (5), MgO (19), and ZnO (7, 9, 20) single crystal surfaces. Few pioneering works examined catalytic performance on ZnO single crystal surfaces, where reaction sites active for the decomposition reaction of 2-propanol (15) and methanol (16) were assigned into defects generated by the reduction of the surfaces. We have reported the catalytic decomposition reaction of formic acid on TiO_2(110), whose surface maintains the original structure during steady-state reaction under DCOOD atmosphere (17, 18).

The acid-base character is one of the most characteristic properties of metal oxides. The selectivity in the catalytic decomposition reaction of formic acid has been used to scale the acid–base property: dehydration over acidic oxide and dehydrogenation over basic oxide (21, 22). Parallel behavior is seen for the decomposition of alcohols (23). Formates are also important as intermediates in the water–gas shift reaction over metal oxides (24). It has been thought that the acid-base character is an intrinsic property on substrates. But in the present study, we report

0021-9517/94 $6.00

a switchover of the reaction paths, from unimolecular dehydration to bimolecular dehydrogenation on TiO_2 (110), when a formic acid molecule participates in the decomposition process of a surface formate.

EXPERIMENTAL

The experiments were carried out in a VG-ESCALAB chamber capable of AES, LEED, XPS, and UPS measurements with a base pressure of 1×10^{-8} Pa. The binding energy in Mg$K\alpha$ XPS was referred to the O(1s) level of the substrate, 530.3 eV (11). UPS spectra were excited with HeI or HeII radiation. TDS spectra were recorded on a quadrupole mass filter (UTI-200) driven by a computer (NEC PC-9801VM).

A special holding device was built to cool and heat the crystal linearly over the range of 100–900 K. A TiO_2(110) wafer ($8 \times 8 \times 1$ mm^3) and a MgO crystal were tightly bound to each other with tantalum wires (0.1 mm ϕ), sandwiching a piece of tungsten mesh (0.03 mm ϕ, 100 mesh, gold plated). The mesh was welded on a couple of electric feedthrus and resistively heated. The feedthrus were attached to a liquid nitrogen reservoir for cooling. The back face of the rutile wafer was coated with gold to ensure a good thermal contact. A chromel–alumel thermocouple was fixed at an edge on the sample surface with ceramic glue (Aronceramic-C). This device allowed a ramping rate of 5 K/s during TDS measurements with electric power below 20 W.

A polished TiO_2(110) wafer obtained from Earth Jewelry Co., Ltd. was oxidized at 1100 K in air for 1 h before cleaning under UHV. The wafer was sputtered with Ar^+ ions of 5 keV and annealed to 800 K in the chamber. A sharp (1×1) pattern was observed in LEED after several cleaning cycles under vacuum. No impurity was detected in AES or in XPS. The crystal turned blue after ten cycles due to a slight reduction of the bulk. Nevertheless, no Ti(3d) emission was detected in HeI UPS, demonstrating a negligible population of reduced Ti^{3+} cations at surface. Oxygen deficiency would result in observable states in Ti(3d) levels (1–3, 24).

DCOOD was used to distinguish D_2 and D_2O in TDS from background H_2 and H_2O. DCOOD of NMR grade (Merck) was outgassed with trap–thaw cycles. A capillary doser (ca. 0.2 mm ϕ) introduced the reactant in front of the sample surface. Effective pressure on the surface was estimated to be 20 times larger than the back pressure. The doser was previously calibrated by dosing CO on a Pd(100) crystal.

A pressure jump method was adopted to measure the rate of catalytic reaction in a steady state with the minimized contribution of the reaction over the holding materials. When the crystal maintained at a reaction temperature is inserted into a stream of formic acid molecules down the doser, catalytic reaction starts on the surface to give jumps in the partial pressure of products. Ideally, the jump height for individual products should correspond to their rate of production. Negative jumps, however, were often observed. Figure 1 shows typical records of reaction in this method. The crystal was brought into the flow at $t = 60$ s and remained until $t = 240$ s. Negative jumps observed in D_2, D_2O, and CO_2 result from the fragmentation of fed DCOOD in the mass filter. When the sample was inserted into the flow, more DCOOD was adsorbed on cold parts of the holder than before and after the insertion. Indeed, the total pressure was decreased during the reaction period. The background levels recorded before and after the reaction period are padded by the fragments of DCOOD. Thus, the true rate for each product was deduced from the difference between two jumps, recorded at a reaction temperature and at 250 K (a blank run). No catalytic reaction was expected at 250 K. The wafer heated at a reaction temperature was assumed not to affect the adsorption on the cooled holder.

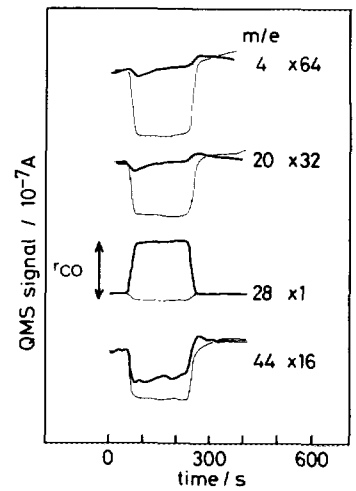

FIG. 1. QMS response in a pressure jump measurement. Thick line: recorded on the sample at 800 K; thin line; recorded at 250 K as a reference. An effective pressure of DCOOD was estimated as 5×10^{-5} Pa on the crystal. r_{CO} corresponds to the rate of CO production (see text).

RESULTS

1. Catalytic Reaction

1.1. Reaction rate and activation energy. Applying the jump method, four products, CO, D_2O, CO_2, and D_2, were observed in the catalytic decomposition of formic acid above 500 K. Neither formaldehyde nor methylformate was detected. The measurements were repeated, changing the surface temperature and the pressure of DCOOD. Figure 2 shows the reaction rate for each product as a function of surface temperature in Arrhenius

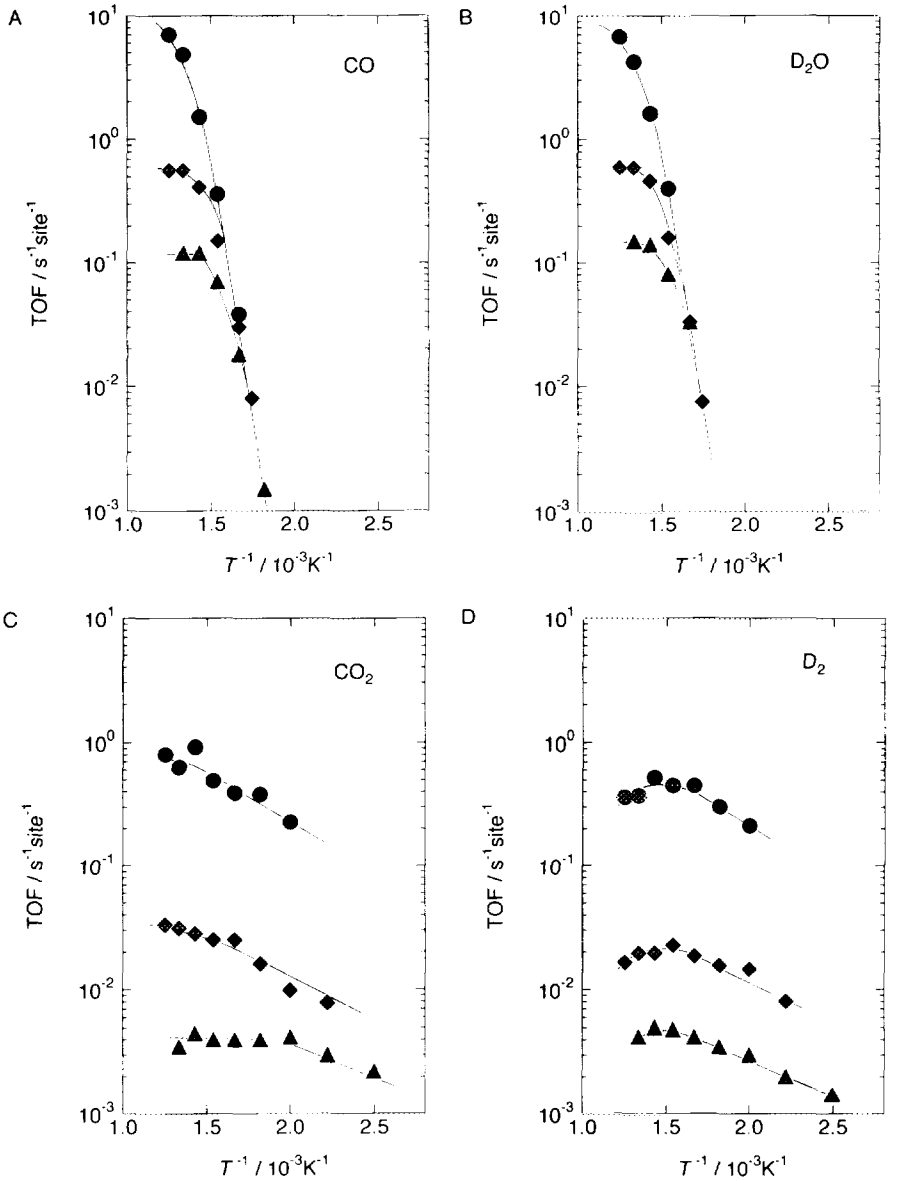

FIG. 2. Rates of the four products in the catalytic decomposition of DCOOD on TiO_2(110). (A) CO; (B) D_2O; (C) CO_2; (D) D_2. Temperature dependence at three typical pressures of formic acid is shown. Circles: 1×10^{-3} Pa; diamonds: 5×10^{-5} Pa; triangles: 4×10^{-6} Pa.

plots. The pumping rate and the relative sensitivity of the mass filter were calibrated by dosing a mixture of given amounts of the four compounds under reaction conditions. The turnover frequency (TOF) is estimated assuming the density of reaction sites to be 2.6×10^{18} m^{-2} on the basis of the coverage of the saturated (2 × 1)-DCOO overlayer (17, 18). None of the products exhibited an induction period, as shown in Fig. 1. The time profiles in partial pressure always gave rapid shifts and plateaus.

There are two reaction paths catalyzed on the (110) surface: dehydration into CO and D_2O, and dehydrogenation into CO_2 and D_2. The dehydration dominated above 650 K, while the dehydrogenation was advantageous at lower temperatures, as shown in Fig. 2. Stoichiometry in dehydration was balanced at every surface temperature examined. The dehydration rates increased with surface temperature and became constant at higher temperatures. An activation energy of 120 ± 10 kJ/mol was observed in the temperature-sensitive region. The transition between the temperature-sensitive and the temperature-insensitive regions occurred at higher temperature with increasing pressure of DCOOD.

The rates of D_2 and CO_2 production exhibited maxima and breaks, respectively. The formation of CO_2 remained

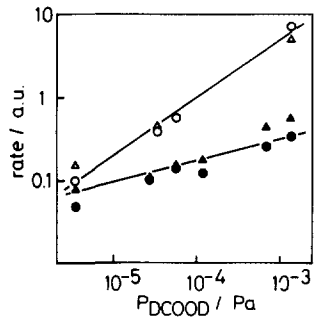

FIG. 3. Dependence of catalytic dehydration rate on the pressure of formic acid. Filled circles: r_{CO} at 650 K; filled triangles: r_{D_2O} at 650 K; open circles: saturated r_{CO}; open triangles: saturated r_{D_2O}.

a slight increase beyond the maxima in the formation of D_2. The activation energy for the dehydrogenation reaction was deduced to be 15 ± 10 kJ/mol in the low-temperature region below the breaks. The maximum temperatures in dehydrogenation correspond with the transition temperatures in dehydration. This suggests that the two reactions are catalyzed via common intermediates.

1.2. Pressure dependence. Figure 3 shows the effects of DCOOD pressure, P_{DCOOD}, on the dehydration rates at constant temperatures. The rates for CO and D_2O were nearly independent of the pressure in the temperature-sensitive region. A small order of 0.2 ± 0.1 was obtained at 650 K. The small dependence on the pressure suggests that the surface is covered with reactants. On the contrary, the rates in the temperature-insensitive region showed a positive order of 0.8 ± 0.2 with respect to the pressure. Furthermore, the transition temperature shifted higher with increasing pressure, as shown in Fig. 2. These results strongly suggest that the surface is no longer saturated with the reactants in the temperature-insensitive region. The switch in reaction order indicates that the rate-determining step shifts from one elementary step to another. The dehydrogenation reaction was of a high order of 0.9 ± 0.1 at 650 K, as shown in Fig. 4.

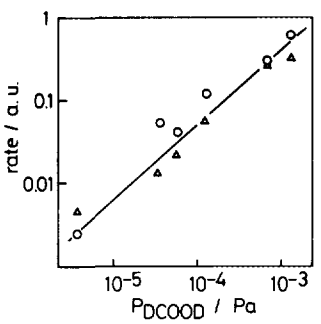

FIG. 4. Dependence of catalytic dehydrogenation rate on the pressure of formic acid at 650 K. Circles: r_{CO_2}; triangles: r_{D_2}.

1.3. Post-reaction LEED. A (2 × 1) ordered structure was observed in post-reaction analysis by LEED, when the sample was cooled under the DCOOD flow after a prolonged reaction. A compatible (2 × 1) pattern was seen on TiO_2(110) exposed to 3 L DCOOD at 250 K, and the pattern will be assigned to the overlayer of 0.5 ML formates adsorbed on TiO_2(110) in the next section. It is hence suggested that TiO_2(110) maintains the original structure during the catalytic reaction; the formation of titanium formate bulk is excluded.

2. Surface Reaction under Vacuum

2.1. TDS. Figure 5 shows TDS spectra recorded on TiO_2(110) after 3 L DCOOD exposure at 230 K (1 L = 1.33 × 10^{-4} Pa s), where a (2 × 1) ordered overlayer was completed. The relative amount of products is listed in Table 1. The relative sensitivity of the mass filter was calibrated. There are three events at 350, 400, and 570 K. DCOOD and D_2O were detected at 300–350 K, followed by a broad desorption peak of D_2 around 400 K. Finally, a mixture of CO, D_2O, CO_2, D_2, and DCOOD was released at 570 K.

The kinetics of the last event were analyzed with heating rates (β) varied in a range of 0.5–4 K/s. The desorption peaks of the five products shifted together in temperature, suggesting that the products are simultaneously released at decomposition of one kind of adsorbates. The results of XPS and UPS will show that the intermediate is formate. The peak temperature of the decomposition products (T_P) exhibited no shift against the initial coverage of formic acid. These kinetic results show that the rate-limiting step of the decomposition is a unimolecular decomposition reaction of the intermediates (formates) on first-order kinetics. Activation energy (E) and preexponential factor (ν) for a first-order process have the relation

$$\ln(T_P^2/\beta) = E/(RT_P) + \ln[E/(R\nu)] \quad [1]$$

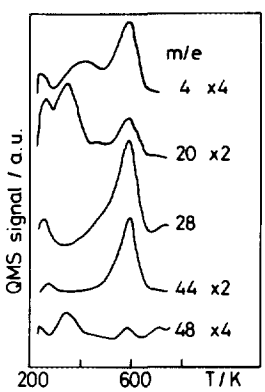

FIG. 5. Thermal desorption spectra following 3 L DCOOD exposure on TiO_2(110) at 230 K. A (2 × 1)-DCOO overlayer was completed. Heating rate was 2 K/s.

TABLE 1

The Relative Amount of Desorption Species in TDS on a (2 × 1)-Formate Overlayer on TiO_2(110)

Temperature (K)	Product	Relative amount[a]
350	DCOOD	16
	D_2O	10
400	D_2	5
570	CO	16
	CO_2	11
	D_2O	5
	D_2	6
	DCOOD	7

[a] The relative sensitivity of the mass filter was corrected.

to T_P and β (25), where R represents the gas constant. The observed values of $\ln(T_P^2/\beta)$ and $1/(RT_P)$ are plotted in Fig. 6. A straight line with $E = 120 \pm 10$ kJ/mol and $\nu = 2 \times 10^{9\pm1}$ s^{-1} fits the data.

2.2. LEED. The clean TiO_2(110) surface gave a (1 × 1) LEED pattern. An exposure to 3 L DCOOD at 180 K increased the intensity of the uniform background with the (1 × 1) pattern unchanged. The background was decreased upon annealing to 200 K. Fractional spots along a (2 × 1) symmetry appeared at 230 K. Further heating at 350 K transformed the (2 × 1) pattern into a (1 × 1) structure, accompanied by the desorption of DCOOD and D_2O. The resultant (1 × 1) pattern was maintained above 800 K. The phase transition was irreversible: the (2 × 1) pattern was not recovered when the transformed (1 × 1) surface was cooled below UHV. In contrast, a small additional exposure to DCOOD easily restored the (2 × 1) order at 300 K.

Under 1×10^{-5} Pa of DCOOD, the (2 × 1) pattern persisted up to 400 K. This shift in the transition temperature demonstrates that the ordered overlayer is equilibrated with DCOOD molecules in the gas phase above 350 K.

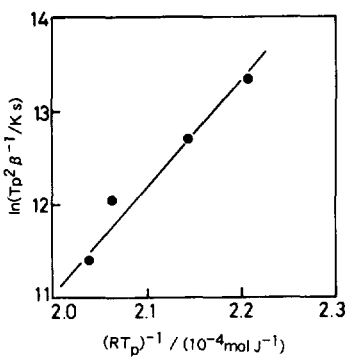

FIG. 6. The shift in the peak temperature for the formate decomposition. The heating rate was varied in TDS.

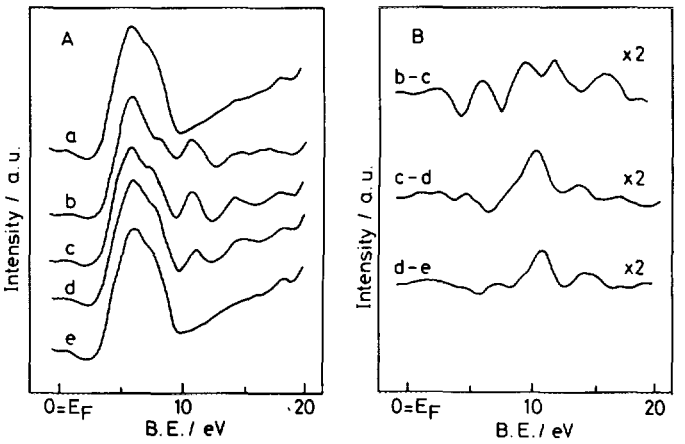

FIG. 7. (A) HeII UPS spectra of formates on TiO_2(110), and (B) the difference spectra. (a) TiO_2(110); (b) exposed to 3 L DCOOD at 180 K. (c), (d), and (e) Successively annealed to 270, 400, and 650 K, respectively. The spectra were taken at 180 K after annealing.

2.3. UPS and XPS. Figure 7A shows typical HeII UPS spectra on TiO_2(110) exposed to DCOOD. The clean surface exhibited a couple of intense emissions at 6 and 8 eV (curve a), which are assigned to O(2*p*) valence bands with bonding or nonbonding character (14). Exposure to 3 L DCOOD at 180 K gave additional peaks. The spectra recorded after successive annealing to 270, 400, and 650 K are presented in curves c, d, and e. These spectra were subtracted in Fig. 7B to examine detailed changes upon annealing, and to distinguish the contribution of molecular and dissociated species.

Curves c − d and d − e exhibit three peaks at 5.0, 10.6, and 14.2 eV in Fig. 7B. They are ascribable to $1a_2 + 6a_1 + 4b_2$, $1b_1 + 3b_2 + 5a_1$, and $4a_1$ orbitals of formates in C_{2v} symmetry on the basis of the assignment of formates on a Cu film (26) and a Cu(110) surface (27). This indicates that the (2 × 1) pattern is due to ordered formates. The emissions of formates gave no shift but decreased in intensity, when the (2 × 1) order disappeared at 350 K.

Molecular species were detected at a lower temperature. Curve b − c consists of four peaks at 6.0, 9.5, 11.9, and 15.9 eV. They are assigned to $10a + 2a''$, $9a + 1a''$, $8a + 7a$, and $6a$ levels of formic acid adsorbed molecularly (26, 27). The intense peaks of formates superimposed on the molecular peaks in curve b. Formic acid gives a mixed layer of molecular and dissociated species at 180 K. Molecularly condensed DCOOD sublimates off the surface below 230 K, corresponding to the decrease of the background in LEED.

No other adsorbates could be distinguished in UPS, though acidic hydrogen atoms resulting from the dissociation of formic acid stay at the surface. They probably react with oxygen anions of the substrate to form hydroxyl

groups, the signal of which species is to be less intense than the emission of formates.

The C(1*s*) emission was observed at 288.9 eV in XPS for a saturated (2 × 1)-formate overlayer at 247 K. This value is acceptable for the carbon atom in a formate. Its relative intensity to the O(1*s*) emission of the lattice oxygen anions was used to estimate the surface density of formates. Orbital cross sections ($\sigma_{O(1s)}/\sigma_{C(1s)} = 2.85$), escape depth of the photoelectrons (1.4 nm for the O(1*s*) level) were considered (11). The transmission of the spectrometer was assumed proportional to 1/KE, where KE is the kinetic energy of the emitted electrons. The coverage of the formates in the (2 × 1) overlayer was determined to be 0.5 ML as a result (11). Here, the coverage is referred to the surface unit cell on clean TiO_2(110); 1 ML corresponds to 5.21×10^{18} m^{-2} (28). When the (2 × 1) surface was annealed at 353 K, the C(1*s*) intensity decreased to 80% without any shift in the binding energy. It means that a formate overlayer of 0.4 ML cannot maintain the (2 × 1) order. No emission was detected in the C(1*s*) region after heating to 650 K.

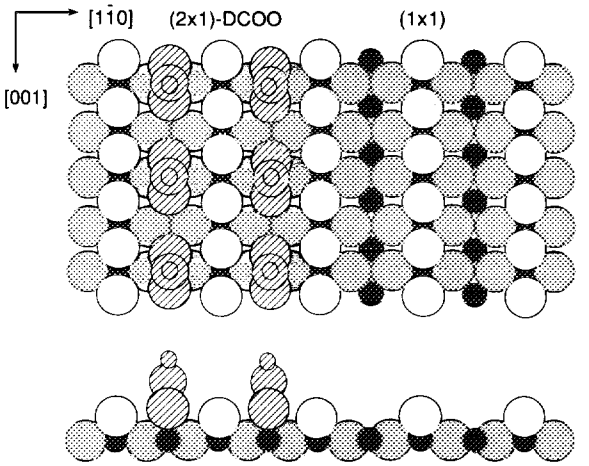

FIG. 8. A model for the TiO_2(110)-(2 × 1)-DCOO overlayer. Open and shaded circles: O^{2-}; filled circles: Ti^{4+}; hatched circles: bridge formate. Formates cover the left side for illustration. Hydroxyl groups are not shown.

DISCUSSION

In the first part of the discussion, noncatalytic surface reactions of adsorbed formic acid are dealt with. The mechanism of the catalytic dehydration reaction is discussed on the basis of the noncatalytic processes. Finally, a bimolecular mechanism is discussed for the catalytic dehydrogenation reaction.

1. Surface Reactions under Vacuum

Adsorbed formic acid gives a mixed adlayer of molecular and dissociated species on TiO_2(110) at 180 K. Molecular DCOOD desorbs below 270 K, leaving formates on the surface according to the UPS results. The hydrogen atoms released in the DCOOD dissociation are likely trapped on oxygen anions of the substrate, O_s, to form hydroxyl groups. There are ridges of oxygen anions with unsaturated coordination on TiO_2(110). They probably have larger affinity to the hydrogen atoms than planar anions have. These processes are summarized as follows: at 180 K,

$$\text{DCOOD(g)} \rightarrow \text{DCOOD(a)}, \quad [2]$$

$$\text{DCOOD(a)} + \text{O}_s \rightarrow \text{DCOO(a)} + \text{O}_s\text{D(a)}, \quad [3]$$

and at 200–230 K,

$$\text{DCOOD(a)} \rightarrow \text{DCOOD(g)}. \quad [4]$$

A model for the (2 × 1) overlayer is illustrated in Fig. 8. All the fivefold Ti^{4+} cations are covered by bridge formates. The three-peak feature in UPS (Fig. 7) and C(1*s*) binding energy (288.9 eV) are assigned to formates. There are three possible coordinations of adsorbed formates. A bidentate formate would result in a distorted, sevenfold coordination around the coordinated titanium cation. A HREELS study reported unidentate formates on ZnO(0001)–Zn (29), where a large separation of 0.325 nm between adjacent Zn cations prefers a unidentate form to bridging coordination. Adjacent fivefold Ti cations to be bridged are separated by a smaller distance of 0.296 nm on TiO_2(110) (28). The oxygen–oxygen distances in formate anions are 0.220–0.227 nm in metal formates, $Ca(HCOO)_2$, $Sr(HCOO)_2$, $Ba(HCOO)_2$, and $Pb(HCOO)_2$ (30). It is reasonable that the formates are adsorbed in a bridge form on TiO_2(110).

Adsorbed formates exhibit no ordered overlayer on MgO(100) (10), ZnO(0001)–Zn (29), and faceted TiO_2(001) (5). Ridges of oxygen atoms run along the [001] direction on TiO_2(110). They are able to arrange the formates in rows. Additionally, each line of formates matches in phase in a (2 × 1) order. The phasing process requires a thermal activation because annealing at 230 K was necessary for the ordering.

The (2 × 1) order disappeared at 350 K, when DCOOD and D_2O were desorbed. The recombination of the formates with the hydroxyl groups,

$$(2 \times 1)\text{-DCOO(a)} + \text{O}_s\text{D(a)} \rightarrow \text{DCOOD(g)} + \text{O}_s, \quad [5]$$

and the disproportionation of the hydroxyl groups,

$$\text{O}_s\text{D(a)} + \text{O}_s\text{D(a)} \rightarrow \text{D}_2\text{O(g)} + \text{O}_s, \quad [6]$$

are responsible for the observed desorption. Similar recombination and disproportionation reactions were reported on faceted TiO_2(001) (5) and ZnO(0001)–Zn (7),

where the protons liberated from O_sD(a) were suggested to trigger off the reactions.

The disordering of the (2 × 1) structure by desorption was irreversible. This means that the less concentrated overlayer of formates cannot maintain the ordered structure even cooled. The formates in the (2 × 1) structure have no freedom of diffusion across the surface, as illustrated in Fig. 8. When a part of formates (0.1 ML) is desorbed, 0.4 ML of formates and 0.2 ML of vacant fivefold Ti cations are left on the surface. The liberated vacant sites promote diffusion to break the long-range order. Surface diffusion of formates seems possible at 350 K. Metal formates have low melting points: 526, 441, and 374 K for NaHCOO, KHCOO, and TlHCOO, respectively (31). This is in line with the fact that the relaxed (1 × 1) surface could recover the (2 × 1) order with a small additional exposure to DCOOD at 300 K.

Desorption of D_2 was observed at 400 K, indicating that a certain amount of D atoms survive. Recombinative desorption of hydrogen was observed at this temperature region on H(D)/Cu_2O(100) (32) and D/TiO_2(110) (33). No molecular hydrogen was detected in TDS following the exposure of facted TiO_2(001) (5), ZnO(0001)–Zn (7), and MgO(100) (10, 19) surfaces to formic acid.

There are 0.4 ML of formates left on the surface after the recombinative desorption. The remaining formates then decomposed at 570 K to a mixture of CO, D_2O, CO_2, D_2, and DCOOD,

$$DCOO(a) \rightarrow CO + D_2O + CO_2 + D_2 + DCOOD. \quad [7]$$

TABLE 2

Kinetic Parameters for the Decomposition of Adsorbed Formates under Vacuum

Substrate	Activation energy (kJ mol^{-1})	Pre-exponential factor (s^{-1})	Ref.
TiO_2(110)	120 ± 10	$2 \times 10^{9\pm1}$	This work
TiO_2 powder	105	3×10^{8}	34
MgO powder	155	5×10^{10}	35
ZnO powder	155	1×10^{10}	36

The rate-determining step of the decomposition reaction is a unimolecular process, since the decomposition is of first-order with respect to the coverage. The desorption peaks of the products shifted together in TDS when the heating rate was varied. This means that one kind of formate decomposes to yield the mixture. If there were several independent paths for dehydration and dehydrogenation with different activation energies, the peaks would shift separately.

The decomposition of formates is a popular process on metal oxides, as shown in Tables 2 and 3. Our activation energy and pre-exponential factor agree with the values reported in Table 2. Contrary to the accordant kinetic parameters, the selectivity in the decomposition products spreads over in Table 3. MgO(100) selectively yields CO, while CO_2 is a dominant product on ZnO(0001)–Zn. The selectivity on rutile crystals sits between the two extreme

TABLE 3

Selectivity (Relative Yield) in the Decomposition of Formates under Vacuum

	Relative amount of products[a]							
Substrate	T_p[b](K)	CO	CO_2	D_2 (H_2)	D_2O (H_2O)	DCOOD (HCOOH)	DCDO (HCHO)	Ref.
TiO_2(110)	570	10	7	4	3	4	0	This work
TiO_2(001) (011)-faceted	560	10	4	(Trace)	0	(4)	0	5
TiO_2(001) (114)-faceted	570	10	5	0	0	(3)	(2)	5
MgO(100)	520	10	0	0	[c]	0	0	19
MgO powder	560	10	0	0	0	0	0	35
ZnO(0001)–Zn	575	10	39	9	0	0	0	7
ZnO(000$\bar{1}$)–Zn	745	10	9–23[d]	[c]	[c]	0	0	9
ZnO(50 $\bar{5}$ 1)	655	10	13[d]	6[d]	3[d]	0	0	9
ZnO(000 $\bar{1}$)–O	560	10	6	[c]	(Trace)	(0)	(0)	20
ZnO powder	550	10	0[e]	4	0	0	0	36

[a] Relative to CO.
[b] Peak temperature in TDS.
[c] Not quantified.
[d] Relative sensitivity of the mass filter was not corrected.
[e] CO_2 is adsorbed on the substrate.

cases. Interestingly, the selectivity in TDS does not reflect catalytic properties. The dehydrogenation reaction of formic acid is selectively catalyzed on MgO and ZnO powder catalysts, and hence those materials are classified as basic oxides. TiO_2 catalysts are more acidic to perform a selective dehydration reaction in a steady state (21). But a certain amount of CO_2 and $H_2(D_2)$ is observed in Table 3. This contradiction tells us that the acid–base character in the catalytic reaction should be distinguished from the selectivity in the noncatalytic surface reaction observed in TDS. Peng and Barteau pointed out that the dehydration/dehydrogenation selectivity in TDS reflects the redox property of substrates; net dehydration does not require reduction of substrate but oxidative dehydrogenation does (19). CO_2 observed in TDS is attributed to oxidative dehydrogenation reactions coupled to the reduction of the substrate. Further, we will state in the next section that the unimolecular decomposition of formates is a selective process to CO and OD on $TiO_2(110)$.

Some secondary reactions are probably responsible for the production of CO_2, D_2, and DCOOD at 570 K:

$$OD(a) + DCOO(a) \rightarrow DCOOD(g) + O(a), \quad [8]$$

$$OD(a) + DCOO(a) \rightarrow D_2(g) + CO_2(g) + O(a), \quad [9]$$

$$OD(a) + OD(a) \rightarrow D_2O(g) + O(a), \quad [10]$$

$$OD(a) + OD(a) \rightarrow D_2(g) + 2O(a). \quad [11]$$

The bimolecular dehydrogenation reaction proposed in the last section is also a possible origin of CO_2 and D_2. If the DCOOD molecule produced in reaction [8] stays near the surface to react with a remaining formate, CO_2 and D_2 are produced.

Formaldehyde is a characteristic product on a (114)-faceted $TiO_2(001)$ surface in TDS (5). Two formates disproportionate on a Ti cation with multiple coordination vacancies (5). The absence of formaldehyde is reasonable on $TiO_2(110)$ because the ideal (110) plane contains no fourfold coordinated cation capable of the disproportionation.

All the results in AES, LEED, XPS, and UPS reveal that formates completely decompose at 570 K to leave a clean $TiO_2(110)$ surface. The disproportionation reaction [6] leads to the loss of oxygen atoms on the substrate. The atomic ratio in the desorption products at 570 K is D : C : O = 36 : 34 : 57, as summarized in Table 1. Comparing the observed ratio with the composition of DCOO, a certain amount of oxygen atoms is consumed to restore the stoichiometry on the surface.

2. *Mechanism of the Catalytic Dehydration Reation*

The rate-determining step for the catalytic dehydration reaction switches over around 700 K, as shown in Fig. 2. The dehydration reaction showed an activation energy of 120 kJ/mol and a pressure dependence of 0.2 order in the temperature-sensitive region at low temperatures. The small order of reaction suggests that adsorbed intermediates nearly cover the surface and their decomposition determines the rate. Indeed, the unimolecular decomposition of formate showed a compatible activation energy of 120 kJ/mol in TDS. Thus the catalytic dehydration reaction is strongly suggested to involve the unimolecular decomposition of formate as a rate-determining step. In other words, the unimolecular decomposition of formate preferentially yields CO(g) and $O_fD(a)$,

$$DCOO(a) \rightarrow CO(g) + O_fD(a), \quad [12]$$

where O_f represents an oxygen atom of formate origin. An acidic deuterium atom of a DCOOD molecule, which encounters the surface in a steady state, reacts with the resultant $O_fD(a)$ to form D_2O,

$$DCOOD(g) + O_fD(a) \rightarrow D_2O(g) + DCOO(a). \quad [13]$$

There can be a rapid scrambling reaction,

$$O_fD(a) + O_s \rightarrow O_f(a) + O_sD(a). \quad [14]$$

The resultant $O_sD(a)$ is also consumed to produce D_2O.

The two reaction steps, [12] and [13], form a catalytic dehydration cycle. One may point out that the decomposition of formate gave not only CO but also D_2O, CO_2, D_2, and DCOOD in TDS. Those products other than CO are ascribed to branching reactions under vacuum [8]–[11]. When step [13] is fast enough to suppress the branching reactions, the catalytic dehydrating cycle works well.

At low temperatures, the decomposition step [12] is rate limiting. The surface is covered with formates, and the rate is of zeroth-order to the pressure of formic acid. With increasing reaction temperature, the decomposition becomes so fast that the whole rate of the reaction is controlled by a short supply of DCOOD on the surface, step [13]. The rate, hence, becomes constant above a certain temperature, and turns to first-order on the pressure. The transition temperature must shift higher with the pressure. This is just what we observed. In this scenario, the turnover frequency (TOF) for the catalytic dehydration reaction approaches the collision frequency of DCOOD molecules in the high-temperature limit. The rate of CO formation turned out to be constant above 650 K at a DCOOD pressure of 5×10^{-5} Pa. The TOF of the unimolecular decomposition step is estimated to be 0.5 s^{-1} at 650 K on the basis of ν and E deduced in TDS. On the other hand, the collision frequency (f) is given as

$$f = P_{DCOOD}/(2\pi mkT)^{1/2}, \quad [15]$$

where m and T are the mass and temperature of the formic acid molecule, respectively, and k is Boltzmann's con-

stant. An adsorption site is assumed to have an area of 3.8×10^{-19} m^2, considering the coverage of the saturated (2×1)-formate adlayer. Thus, the frequency is estimated as 0.5 molecule s^{-1} site^{-1} at $P_{DCOOD} = 5 \times 10^{-5}$ Pa and $T = 300$ K. The estimated TOF agrees with f, which supports our mechanism.

Polycrystalline TiO_2 powder is known to be a dehydration catalyst (21, 34, 37). Munuera (34) studied the catalytic decomposition of HCOOH on TiO_2 powder above 630 K at a pressure of 8×10^2 Pa, and observed a selectivity ca. 90% for dehydration with zeroth-order kinetics. An activation energy of 105 kJ/mol and a pre-exponential factor of 2×10^{27} molecules m^{-2} s^{-1} were also reported (34). The latter corresponds to 7×10^8 molecules site^{-1} s^{-1}. These values are compatible with ours. We suggest that the dehydration reaction on the polycrystalline catalyst proceeds in the same mechanism as that on rutile (110), though Munuera proposed that the formation of water from hydroxyls limits the rate in his original report (34).

In reaction step [12], the D atom in a formate shifts to one of the formate oxygen atoms. The C–D bond and one of the C–O bonds break as a result. The produced CO is immediately released from the surface. This set of bond rearrangements triggered by the intramolecular transfer of the D atom seems possible as an elementary step. A lattice oxygen O_s might also receive the D atom of the formate directly. However, if the D atom was transferred directly to O_s, CO_2 rather than CO would be preferably formed.

Formates on transition metal surfaces decompose at lower temperatures (300–500 K) than on TiO_2(110), where the hydrogen atom is taken off by the substrates (21, 38). It was suggested that the wagging motion of the adsorbed formate which brings the hydrogen atom close to the metal surfaces promotes the decomposition (38). There are two possible reasons why the transfer of the D atom of formate to the lattice oxygen is obstructed on TiO_2(110): Rutile has smaller affinity to the hydrogen atoms, and the wagging vibration could be prohibited by the ridges on TiO_2(110).

Another mechanism of dehydration was proposed on Al_2O_3 and SiO_2 catalysts (39). Proton transfer from hydroxyls on the substrates to molecularly adsorbed formic acid initiates a catalytic dehydration reaction. This process is an analog of acidic catalysis in liquid phase. The protonated mechanism may be possible on a passive surface, such as ZnO(000$\bar{1}$)–O. Formic acid cannot find an active cation on an O-terminated polar surface; only desorption of molecular species was observed in TDS (7).

3. *Mechanism of the Catalytic Dehydrogenation Reaction*

The rate of D_2 formation has maxima in the Arrhenius plots of Fig. 2. The maximum temperatures correspond to the transition temperatures in the dehydration. The decrease in the rate at higher temperatures is ascribed to the decrease of formate coverage, where the formates are consumed in the dehydrating decomposition so fast that the coverage decreases with temperature. The observed maximum this suggests that the dehydrogenation reaction requires surface formates. The formates, however, decompose to CO(g) and O_fD(a) by themselves, as stated above. Another mechanism must be considered for the dehydrogenation reaction.

Figure 4 shows first-order kinetics for the dehydrogenation reaction at 600 K. Since the coverage of formates is nearly saturated at 600 K, the observed first-order dependence suggests that a DCOOD molecule further participates in the rate-determining step of the dehydrogenation reaction. This was numerically simulated on the following model. Formic acid molecules are adsorbed on vacant sites with a rate of $f(1 - 2\theta)$, where θ is the coverage of formate,

$$\mathrm{DCOOD(g)} + \mathrm{O_s} \xrightarrow{f(1-2\theta)} \mathrm{DCOO(a)} + \mathrm{O_sD(a)}. \quad [16]$$

The factor of two comes from the saturation coverage of 0.5 ML for formates. The formates unimolecularly decompose to the dehydrated products with a rate r_1,

$$\mathrm{DCOO(a)} \xrightarrow{r_1} \mathrm{CO(g)} + \mathrm{O_fD(a)}, \quad [17]$$

where

$$r_1 = 2k_1\theta. \quad [18]$$

The rate constant k_1 is given by

$$k_1 = \nu_1 \exp[-E_1/(RT)]. \quad [19]$$

The resultant O_fD(a) rapidly reacts with another DCOOD molecule to yield D_2O and a formate. Thus a catalytic cycle for the dehydration reaction is completed. As a competitive path, the formate reacts with a DCOOD molecule to give the dehydrogenated products

$$\mathrm{DCOO(a)} + \mathrm{DCOOD(g)} \xrightarrow{r_2} \mathrm{CO_2(g)} + \mathrm{D_2(g)} + \mathrm{DCOO(a)}. \quad [20]$$

The dehydrogenation rate r_2 is thereby given by the product of the collision frequency f and the coverage, multiplied with an Arrhenius-type probability for reaction,

$$r_2 = 2f\theta \exp[-E_2/(RT)]. \quad [21]$$

The bimolecular dehydrogenation reaction consumes no formate apparently. The coverage is given in the balance of $f(1 - 2\theta)$ and r_1,

$$\theta = f/[2(f + k_1)]. \quad [22]$$

The TOFs for both reactions are calculated on this model with the observed parameters $\nu_1 = 2 \times 10^9\ s^{-1}$, $E_1 = 120$ kJ/mol, $E_2 = 15$ kJ/mol, and $f = 0.5\ s^{-1}\ site^{-1}$. The results shown in Fig. 9 successfully represent the observed kinetic features. A bimolecular dehydrogenation reaction of a formate with an impinging or weakly adsorbed DCOOD molecule is thus proposed. In Fig. 2, CO_2 still increased at high temperature, whereas D_2 formation decreased. The variation of the formate coverage explains the deviation. The oxidative dehydrogenation reaction coupled to the reduction of the substrate,

$$DCOOD + O_s \rightarrow CO_2(g) + D_2O(g), \quad [23]$$

is responsible for the excess production of CO_2. Reaction [9] branching to CO_2 can take place in supply-limited situations at high temperatures. Note that CO_2 was detected twice as much as D_2 in TDS.

Reaction [20] is not an elementary step. It is likely that the acidic D atom of the DCOOD molecule reacts with the D atom of the formate to form D_2, and the resultant CO_2 desorbs at once.

Dehydrogenation reaction on a metal oxide catalyst usually has an activation energy higher than that for dehydration reaction on the catalyst (21). However, the observed activation energy, 15 kJ/mol, is much smaller than that for the dehydration reaction (120 kJ/mol). The participation of a DCOOD molecule switches over the reaction paths from dehydration to dehydrogenation, decreasing the activation energy. If the formates react with adsorbed DCOOD molecules equilibrated with gas phase, the apparent activation energy becomes smaller than the true barrier by the heat of adsorption of the molecular species.

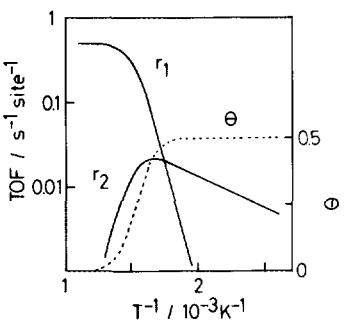

FIG. 9. Reaction rates simulated as a function of reaction temperature with a collision frequency of 0.5 s^{-1} $site^{-1}$. r_1: dehydration; r_2: dehydrogenation; θ: the coverage of formates.

Although TiO_2 powder is a selective catalyst for the dehydration (21, 34, 37), the present study shows that $TiO_2(110)$ favors the dehydrogenation at low temperatures. There are two possible reasons for the discrepancy. If the dehydrogenation reaction is characteristic for the (110) plane of rutile, polycrystalline crystals are disadvantageous. However, crystallographic studies on faceted (001) (6, 40) and reconstructed (100) $-$ (1 $\times$ 3) surfaces (41) reveal that the (110) plane is the most stable surface on rutile crystal. It is unlikely that the (110) plane is a minority on rutile powders. Another crystal form, anatase, is favorable depending on the history of catalysts, which complicates the situation on TiO_2 powders. The other possible origin is a restricted reactivity of saturated overlayers of formates. There is no vacant cation left on the (2 $\times$ 1)-formate structure, whereas 0.2 ML of fivefold coordinated cations remain vacant in the relaxed overlayer. If a vacant cation and/or certain space around a formate are required to form the reaction complex for the bimolecular dehydrogenation, a complete (2 $\times$ 1)-formate phase suppresses the dehydrogenation reaction. According to our LEED observation, the (2 $\times$ 1) phase is equilibrated with the gas phase and cannot persist under the reaction conditions here. Higher pressures employed in usual catalytic studies are capable of forming close-packed adlayers of formates. Catalytic study under higher pressures will distinguish the two possibilities on a $TiO_2(110)$ single crystal surface.

Several studies have reported bimolecular processes in the dehydrogenation reaction of formates. A bimolecular reaction of a formate with an impinging formic acid molecule was proposed for the dehydrogenation reaction on ZnO and MgO powder catalysts (42). Co-adsorbed water molecules promote the dehydrogenation reaction of formates on MgO (35), ZnO (36), and Rh-doped CeO_2 (43) catalysts, decreasing activation energy.

It is interesting to relate the unimolecular dehydration and the bimolecular dehydrogenation on $TiO_2(110)$ to the reported processes on polycrystalline oxide catalysts. Further studies of catalysis on well-defined surfaces, such as MgO(100), ZnO(0001)–Zn, and ZnO(000$\bar{1}$)–O, will help us address the point.

CONCLUSIONS

(i) The unimolecular decomposition of adsorbed formates at 570 K is a selective process to form CO and OD(a) on $TiO_2(110)$, though CO_2, D_2, and DCOOD are also observed in TDS. The latter products come from branching reactions successive to the selective decomposition.

(ii) Catalytic dehydration reaction of formic acid proceeded on TiO_2(110) by the cycle of two steps: the unimolecular decomposition of formate and the subsequent production of water.

(iii) Catalytic dehydrogenation reaction of formic acid was found to be a main reaction on TiO_2(110) at low temperatures. This reaction is catalyzed by a bimolecular process between a formate and a formic acid molecule.

(iv) The switchover in the reaction paths from dehydration to dehydrogenation with the different mechanisms on a surface suggests a new aspect of acid–base catalysis besides the intrinsic property of oxide surfaces.

REFERENCES

1. Henrich, V. E., *Prog. Surf. Sci.* **14,** 175 (1983).
2. Heiland, G., and Lüth, H., "The Chemical Physics of Solid Surfaces and Heterogeneous Catalysis," Vol. 3, Chap. 4. Elsevier, Amsterdam, 1984.
3. Henrich, V. E., and Cox, P. A., "The Surface Science of Metal Oxides." Cambridge Univ. Press, Cambridge, 1993.
4. Idriss, H., Kim, K. S., and Barteau, M. A., *J. Catal.* **139,** 119 (1993).
5. Kim, K. S., and Barteau, M. A., *Langmuir* **6,** 1485 (1990).
6. Kim, K. S., and Barteau, M. A., *J. Catal.* **125,** 353 (1990).
7. Vohs, J. M., and Barteau, M. A., *Surf. Sci.* **176,** 91 (1986).
8. Vohs, J. M., and Barteau, M. A., *Surf. Sci.* **201,** 481 (1988).
9. Akhter, S., Cheng, W. H., Lui, K., and Kung, H. H., *J. Catal.* **85,** 437 (1984).
10. Onishi, H., Egawa, C., Aruga, T., and Iwasawa, Y., *Surf. Sci.* **191,** 479 (1987).
11. Onishi, H., Aruga, T., Egawa, C., and Iwasawa, Y., *Surf. Sci.* **193,** 33 (1988).
12. Onishi, H., Aruga, T., Egawa, C., and Iwasawa, Y., *Surf. Sci.* **199,** 54 (1988).
13. Onishi, H., Aruga, T., Egawa, C., and Iwasawa, Y., *J. Chem. Soc., Faraday Trans. 1* **85,** 2597 (1989).
14. Tsukada, M., Adachi, H., and Satoko, C., *Prog. Surf. Sci.* **14,** 113 (1983).
15. Berlowitz, P., and Kung, H. H., *J. Am. Chem. Soc.* **108,** 3532 (1986).
16. Vest, M. A., Lui, K. C., and Kung, H. H., *J. Catal.* **120,** 231 (1989).
17. Onishi, H., Aruga, T., and Iwasawa, Y., *J. Am. Chem. Soc.,* **115,** 10460 (1993).
18. Onishi, H., Aruga, T., and Iwasawa, Y., *Shokubai* **34,** 428 (1992).
19. Peng, X. D., and Barteau, M. A., *Catal. Lett.* **7,** 395 (1990).
20. Ludvikkson, A., Zhang, R., and Campbell, C. T., in preparation.
21. Mars, P., Scholten, J. J. F., and Zwietering, P., *Adv. Catal.* **14,** 35 (1963).
22. Scholten, J. J. F., Mars, P., Menon, P. G., and van Hardereld, R., *in* "Proceedings, 3rd International Congress on Catalysis, Amsterdam, 1964," Vol. 2, p. 881. Wiley, New York, 1965.
23. Szabo, Z. G., *J. Catal.* **6,** 458 (1966).
24. Chung, Y. W., Lo, W. J., and Somorjai, G. A., *Surf. Sci.* **64,** 588 (1977).
25. Redhead, P. A., *Vacuum* **12,** 203 (1962).
26. Joyner, R. W., and Roberts, M. W., *Proc. R. Soc. London,* A **350,** 107 (1976).
27. Bowker, M., and Madix, R. J., *Surf. Sci.* **102,** 542 (1981).
28. Wyckoff, R. W. G., *in* "Crystal Structure," 2nd ed., Vol. 1, p. 251. Wiley, New York, 1965.
29. Petrie, W. T., and Vohs, J. M., *Surf. Sci.* **245,** 315 (1991).
30. Wyckoff, R. W. G., *in* "Crystal Structure," 2nd ed., Vol. 5, p. 121. Wiley, New York, 1966.
31. CRC Handbook of Chemistry and Physics 63rd (1982–83), CRC Press, Boca Raton, Florida.
32. Schulz, K. H., and Cox, D. F., *Surf. Sci.* **278,** 9 (1992).
33. Onishi, H., Aruga, T., and Iwasawa, Y., in preparation.
34. Munuera, G., *J. Catal.* **18,** 19 (1970).
35. Shido, T., Asakura, K., and Iwasawa, Y., *J. Catal.* **122,** 55 (1990).
36. Shido, T., and Iwasawa, Y., *J. Catal.* **129,** 343 (1991).
37. Trillo, J. M., Munuera, G., and Criado, J. M., *Catal. Rev.* **7,** 51 (1972).
38. Madix, R. J., *Adv. Catal.* **29,** 1 (1980).
39. Fukuda, K., Noto, Y., Onishi, T., and Tamaru, K., *Trans. Faraday Soc.* **63,** 3072 (1967).
40. Firment, L. E., *Surf. Sci.* **116,** 205 (1982).
41. Zschck, P., Cohen, J. B., and Chung, Y. W., *Surf. Sci.* **262,** 395 (1992).
42. Noto, Y., Fukuda, K., Onishi, T., and Tamaru, K., *Trans. Faraday Soc.* **63,** 3081 (1967).
43. Shido, T., and Iwasawa, Y., *J. Catal.* **141,** 71 (1993).